Source apportionment of PM2.5 oxidative potential in an East Mediterranean site

Marc Fadel, Dominique Courcot, Gilles Delmaire, Gilles Roussel, Charbel Afif, Frédéric Ledoux

Source apportionment of $PM_{2.5}$ oxidative potential in an East Mediterranean site

Marc Fadel[a,b], Dominique Courcot[b], Gilles Delmaire[c], Gilles Roussel[c], Charbel Afif [a,d], Frédéric Ledoux[b,*]

[a]Emissions, Measurements, and Modeling of the Atmosphere (EMMA) Laboratory, CAR, Faculty of Sciences, Saint Joseph University, Beirut, Lebanon

[b]Unité de Chimie Environnementale et Interactions sur le Vivant, UCEIV UR4492, Université du Littoral Côte d′Opale (ULCO), Dunkerque, France

[c]Laboratoire d'Informatique Signal et Image de la Côte d'Opale (LISIC), Université du Littoral Côte d'Opale, F – 62228, Calais, France

[d]Climate and Atmosphere Research Center, The Cyprus Institute, Nicosia, Cyprus

*Corresponding author: frederic.ledoux@univ-littoral.fr

Abstract:

This study aimed to evaluate the oxidative potential (OP) of $PM_{2.5}$ collected for almost a year in an urban area of the East Mediterranean. Two acellular assays, based on ascorbic acid (AA) and dithiothreitol (DTT) depletion, were used to measure the OP. The results showed that the mean volume normalized OP-AA_v value was 0.64 ± 0.29 nmol·min^{-1}·m^{-3} and the mean OP-DTT_v was 0.49 ± 0.26 nmol·min^{-1}·m^{-3}. Several approaches were adopted in this work to study the relationship between the species in $PM_{2.5}$ (carbonaceous matter, water-soluble ions, major and trace elements, and organic compounds) or their sources and OP values. Spearman correlations revealed strong correlations of OP-AA_v with carbonaceous subfractions as well as organic compounds while OP-DTT_v seemed to be more correlated with elements emitted from different

anthropogenic activities. Furthermore, a multiple linear regression method was used to estimate the contribution of $PM_{2.5}$ sources, determined by a source-receptor model (Positive Matrix Factorization), to the OP values. The results showed that the sources that highly contribute to the $PM_{2.5}$ mass (crustal dust and ammonium sulfate) were not the major sources contributing to the values of OP. Instead, 69% of OP-AA_v and 62% of OP-DTT_v values were explained by three local anthropogenic sources: Heavy Fuel Oil (HFO) combustion from a power plant, biomass burning, and road traffic emissions. As for the seasonal variations, higher OP-AA_v values were observed during winter compared to summer, while OP-DTT_v did not show any significant differences between the two seasons. The contribution of biomass burning during winter was 33 and 34 times higher compared to summer for OP-AA_v and OP-DTT_v, respectively. On the other hand, higher contributions were observed for HFO combustion during summer.

Keywords: PM oxidative potential, source apportionment, multiple linear regression, correlation analysis with chemical composition, seasonal variations.

Introduction

Air pollution is considered as one of the major environmental challenges and poses a major threat to health and climate. According to the World Health Organization, 99% of people worldwide were living in areas where air quality exceeded the WHO guidelines in 2019 (WHO, 2021). It is estimated that the attributable excess mortality rate from ambient air pollution is about 8.8 million per year (Lelieveld et al., 2019). Among the different air pollutants, particulate matter with an aerodynamic diameter less than 2.5 µm ($PM_{2.5}$) can be easily inhaled into the lungs and might cause diverse health effects especially cardiovascular and respiratory diseases (Anderson et al., 2012; Lelieveld and Münzel, 2020; Xing et al., 2016). The exact mechanisms of toxicity induced by exposure to PM are still poorly understood. Toxicological studies have shown that the exposure to PM could induce oxidative stress by stimulating cells to produce reactive oxygen species (ROS) in excess of the antioxidant capacity of the body (Ayres et al., 2008; Bates et al., 2015). This imbalance triggers a cascade of effects such as inflammation, DNA damage, and cell death (Becker et al., 2005; Wang et al., 2019). Additionally, the toxicological effects due to the induction of oxidative stress by PM is related to their physico-chemical characteristics such as surface properties and their chemical composition (Crobeddu et al., 2017). Hence, the oxidative potential (OP) of PM has been found to be a practical indicator for the evaluation of the oxidative capacity of PM components as a whole (Crobeddu et al., 2017). According to Daellenbach et al. (2020) and Fakhri et al. (2023), if the OP is found to be related to major health impacts, it might be more effective to control specific OP sources rather than overall particulate mass. Recent papers showed that the correlation between acellular OP and intracellular toxicity is site-dependent following the sources acting on a specific site

(Guascito et al., 2023; Weber et al., 2021; Xu et al., 2020). Therefore, further studies are needed to investigate the impact of the emission sources on both aspects.

Recently, the development of different acellular assays has led to a rise in OP measurements worldwide and their inclusion in epidemiological studies (Serafeim et al., 2023). The most common ones include electron spin resonance (OP-ESR) that measures the generation of hydroxyl radicals, dithiothreitol (OP-DTT), ascorbic acid (OP-AA) and glutathione (OP-GSH) assays that measure the depletion rate of proxies for cellular reductants or antioxidants (Bates et al., 2019; Guo et al., 2020). Among those, OP-AA and OP-DTT are widely used and are based on spectrophotometric kinetic methods (Bates et al., 2019). The OP-DTT assay measures the depletion rate of dithiothreitol, a chemical reactant used as a substitute of cellular reductants owing to its sulfhydryl groups (Cho et al., 2005). While the OP-AA assay measures the ability of PM to deplete antioxidants (ascorbic acid in this case) in the respiratory tract lining fluid (RTLF) (Mudway et al., 2004). These depletion rates are proportional to the generation rate of ROS and the ability of PM to contribute to ROS overproduction. Up until today, there is no standard methodology to measure oxidative potential in order to fully determine the ROS generation variations (Janssen et al., 2014; Weber et al., 2021). This methodology should include different tests due to their different sensitivities to PM components (Ayres et al., 2008). The current state of knowledge regarding the correlation between species and the different OP assays is not enough to reach a conclusion about the specificity of the tests to classes of compounds. Nevertheless, an OP assessment based on the OP-AA and OP-DTT assays seems appropriate when considering different families of PM components due to the complementarity between these assays (Guo et al., 2020). However, the study of the relationship between OP values and PM sources is sometimes limited since PM species and elements contributing to OP values can

be emitted by several sources. Additionally, few studies tried to determine OP values produced by specific sources such as biomass burning and urban traffic (Bates et al., 2015; Saffari et al., 2014). Therefore, assuming that OP is a predictive metric of the PM toxicity, it has become increasingly important to link the OP values to PM sources in order to identify the sources with the greatest possible impact. Bates et al. (2015) and Weber et al. (2018) developed methodologies for the evaluation of the contributions of the sources using a multiple linear regression approach in order to assign OP-AA and OP-DTT values for different sources obtained by source apportionment application. More recently, Borlaza et al. (2021) compared a non-linear modelling technique (Multilayer perceptron neural network analysis - MLP) to the multiple linear regression model and showed similarities between the results of the two models with some improvements in the OP prediction with the MLP model when local features or non-linear effects occur.

In this context, the objectives of this research were to examine the oxidative potential of $PM_{2.5}$ measured using AA and DTT assays, to study the relationship between the $PM_{2.5}$ chemical components (carbonaceous, ionic, elemental, and organic) and OP results, and to conduct a source apportionment of $PM_{2.5}$ OP. The source apportionment of $PM_{2.5}$ at the site was previously presented in Fadel et al. (2023). This study will try to contribute to filling the lack of knowledge regarding OP measurements and their attribution to common sources found in the East Mediterranean and the Middle East region.

1 Materials and methods

1.1 $PM_{2.5}$ sampling

$PM_{2.5}$ sampling was conducted at Zouk Mikael (ZK), an urban site under industrial influence in Lebanon. Detailed information about the sampling site and the sample collection were presented in Fadel et al. (2021). The ZK site (33°57'57.07''N; 35°37'09.46''E) is highly urbanized with a residential density of 4,200 inhabitants/km^2, located at 1.2 km of a congested highway linking the capital Beirut to the North of Lebanon **(Figure 1)**. This site also encompasses the biggest power plant in the country which runs on Heavy Fuel Oil (HFO).

$PM_{2.5}$ samples were collected for 24 hours on pre-cleaned Quartz microfibres filters (150 mm, Fiorini, France) every third day from 13th of December 2018 to 15th of October 2019, using a high-volume sampler (CAV-A/mb, MCV S.A., Spain) operating at 30 m^3/h. A total number of 98 loaded filters and 8 field blanks were collected.

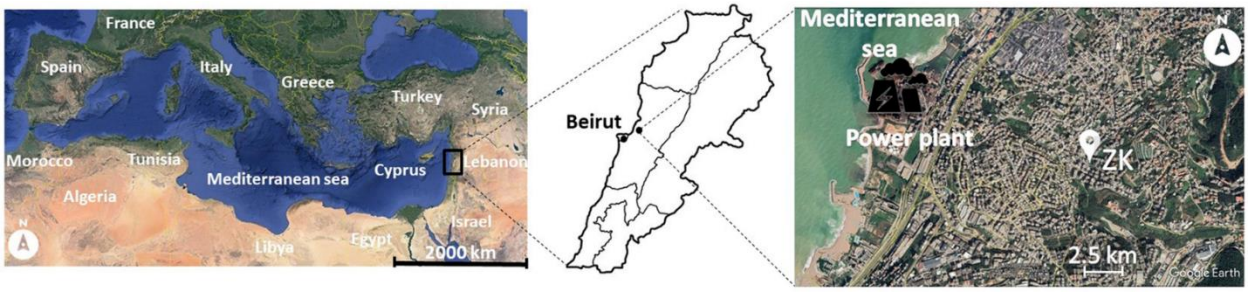

Figure 1: Location of the sampling site at Zouk Mikael (ZK), Lebanon (modified from Google Earth)

1.2 $PM_{2.5}$ concentrations and chemical characterization

Detailed information regarding the determination of $PM_{2.5}$ concentrations as well as the chemical characterization can be found in the supplementary material and in our previous publications

(Fadel et al., 2023; 2022; 2021). Briefly, the $PM_{2.5}$ concentration was determined based on the standard gravimetric method EN 12341:2014 by weighing filters before and after sampling in a temperature (20 ± 0.5°C) and humidity (50 ± 5%) controlled room.

Various analytical methods were used to analyze different chemical fractions of $PM_{2.5}$. The carbonaceous sub-fractions (OC and EC) were analyzed by a Sunset Laboratory analyzer implementing the EUSAAR2 temperature protocol (Cavalli et al., 2010). Organic compounds such as Polycyclic Aromatic Hydrocarbons (PAHs), alkanes, hopanes, levoglucosan, carboxylic acids, isoprene and α-pinene oxidation products were analyzed by gas chromatography coupled to a mass spectrometer GC/MS (ISQ 7000, Thermo Scientific, United States of America) using the method described in Fadel et al. (2021). The analysis of major and trace elements was performed by an Inductively Coupled Plasma-Atomic Emission Spectrometry (ICP-AES, iCAP 6000 series, Thermo Scientific, United Kingdom), and an ICP-Mass Spectrometry (ICP-MS, Agilent 7900, Varian, United States of America), respectively using the method described in Ledoux et al. (2006b) and Fadel et al. (2022). Finally, water-soluble ions were analyzed by ion chromatography (Dionex™ ICS-900, Thermo Scientific, United Kingdom) following the method presented by Ledoux et al. (2006a) and Fadel et al. (2023).

1.3 $PM_{2.5}$ oxidative potential evaluation

The method used for the assessment of the oxidative potential using AA and DTT assays was detailed in Moufarrej et al. (2020) and will be briefly presented here. The leaching agent used for the $PM_{2.5}$ extraction is the Gamble's solution (pH=7.4), a simulated lung fluid (SLF) that reflects the composition of the interstitial fluid in the deep lung. The composition of the Gamble's

143 solution as well as the order of mixing of the components can be found in Colombo et al. (2008)
144 and in **Table S1.** For each sample, a punch of the filter (19 mm diameter) was extracted by 5 mL
145 of the Gamble's solution in a glass tube. The tubes were then placed in a heated orbital shaker
146 for 24 h at 37°C, at a speed of 250 oscillations per min. The extracted solutions were then filtered
147 on 0.45 µm nylon filters, and stored at -20°C until OP analysis.

148 The measurement of DTT depletion was carried out in 96 well black plates with clear flat
149 bottom. In each well of the plate, 40 µL of the PM leachate (or the Gamble's solution used as
150 blank or a filter field blank or 1,4-naphtoquinone used as positive control) was added to 120 µL
151 of phosphate buffer solution (pH = 7.4) before placing the plate under shaking for 10 min at
152 37°C. Then, the oxidation reaction was initiated by adding 25 µL of DTT (0.4 mM) and the
153 estimation of the remaining DTT was done by adding 15 µL of 5,5-dithio-bis-(2-nitrobenzoic
154 acid) (DTNB) in the wells at different times of reaction between the PM leachate and DTT at
155 37°C. The remaining DTT reacts with DTNB and is converted to 2-nitro-5-thiobenzoic acid
156 (TNB). The absorbance of TNB was measured 10 min after the last DTNB addition at 37°C and
157 at 412 nm.

158 The OP-AA assay was done in 96 well plates with UV-transparent flat bottom. In each well, 160
159 µL of PM extract were added and then the plate was incubated at 37°C for 10 min under shaking.
160 Then, 40 µL of the AA solution (1 mM) was added to the extract and incubated for 1 min before
161 placing it in the spectrophotometer. The absorbance of the remaining AA was measured at 265
162 nm every 2 min for 2 hours.

163 The AA or DTT depletion rates were determined by considering the slope of the linear
164 regression of the remaining AA or DTT, respectively versus time. For each $PM_{2.5}$ sample, OP-
165 AA or OP DTT values (in $nmol \cdot min^{-1}$) were corrected by subtracting the slope value of the field

blank filter. Then, the values were normalized to the mass of PM ($OP\text{-}AA_m$ and $OP\text{-}DTT_m$ expressed in $nmol \cdot min^{-1} \cdot \mu g^{-1}$) and to the volume of air ($OP\text{-}AA_v$ and $OP\text{-}DTT_v$ expressed in $nmol \cdot min^{-1} \cdot m^{-3}$). For both assays, samples were analyzed in triplicates and the relative standard deviation was below 7% for OP AA and below 10% for OP DTT.

1.4 Data processing

1.4.1 Source apportionment of $PM_{2.5}$

The identification and the quantification of the contribution of $PM_{2.5}$ sources was done using the USEPA PMF 5.0 model (Paatero and Tapper, 1994). The detailed results regarding the identified sources at ZK site, the source profiles, and their contribution to $PM_{2.5}$ can be found in our previous publication (Fadel et al., 2023). Briefly, a selection of 32 species including the carbonaceous sub-fractions (OC, EC), major ions (Cl^-, SO_4^{2-}, NO_3^-, Na^+, and NH_4^+), a set of elements (Mg, Al, Ca, Fe, K, Ni, Ti, Cu, Sb, and Sn), and different organic tracers (levoglucosan, hexa- and octadecanoic acids, isoprene and α-pinene oxidation products, 17α(H)-21β (H)-hopane, C_{20}, C_{21}, C_{24}, C_{25}, C_{27}, C_{29}, and C_{31} alkanes) were added into the model. A twelve-factor solution was retained and the source categories were presented in **Table 1**.

The measured concentrations of $PM_{2.5}$ as well as the added species and the values reconstructed were strongly correlated with regression slopes higher than 0.85 and determination coefficients (R^2) higher than 0.83. Additionally, bootstrap analyses and DISP diagnostics indicated a good model fit for the twelve-factor solution.

1.4.2 Correlation analysis

In order to analyze the correlations between OP data and $PM_{2.5}$ components, statistical tests were used after assessing the normality of the variables. The Shapiro-Wilk test was performed to evaluate the normality of the distributions. Most of the variables were not normally distributed ($p<0.001$). Therefore, the Spearman correlation coefficient, a non-parametric test to study the correlations was chosen. Two levels of significance were generally applied, $p<0.05$ for 95% confidence, and $p<0.01$ for 99% confidence. The seasonal variability of the OP values was analyzed using the Mann-Whitney statistical test.

1.4.3 Oxidative potential apportionment method

A multiple linear regression method has been used in order to estimate the contributions of PM sources to OP. The method is based on the assumption that the OP values are linearly related to the contributions of the sources using the following equation (Weber et al., 2018) (Eq.1):

$$OP_{obs} = \sum_{i=1}^{n} C_{i-PM} \times \beta_i + \varepsilon \qquad (Eq.1)$$

Where OP_{obs} is the observed OP_v value matrix expressed in $nmol \cdot min^{-1} \cdot m^{-3}$, $C_{i\text{-}PM}$ is the concentration of PM attributed to the source *i* in the source contribution matrix expressed in $\mu g \cdot m^{-3}$, β_i represents the intrinsic OP of the source ($nmol \cdot min^{-1} \cdot \mu g^{-1}$), and ε is a residual term (in $nmol \cdot min^{-1} \cdot m^{-3}$) that accounts for the misfit between the observed and the modeled data. The MLR was done by imposing the intercept equal to zero.

A weighted least square regression (WLS) was adopted in order to take into consideration the uncertainties of the OP measurements. The input data for this model are the contributions of the

sources resulting from the PMF results for the ZK site, and the values of OP-AA_v and OP-DTT_v along with their corresponding uncertainties. The latter were calculated at 2σ based on the RSD of the triplicates, the uncertainty related with the sampling instrumentation, and the uncertainties associated with the experimental procedures.

Once the initial run is done and values of intrinsic OP are calculated, sources with negative intrinsic OP that are statistically unsignificant at 5% level ($p > 0.05$) were removed from the input data and the MLR was run again without these sources.

Afterwards, a bootstrap analysis on the MLR model is applied to evaluate the variability of the obtained intrinsic OP results. This method creates sets of bootstrap data constructed by randomly selecting blocks of observations from the initial dataset. The size of the blocks is calculated according to Politis and White (2004) and was taken in this case as 5 samples per block. 100 bootstrap runs were randomly performed to ensure the robustness of the results. The obtained intrinsic OP values were presented in a boxplot presenting the median and the percentiles 5, 25, 50, 75, and 90 **(Figure 2).**

2 Results and discussions

2.1 $PM_{2.5}$ composition and source contribution

The concentrations of the different $PM_{2.5}$ components (OC, EC, water-soluble ions, elements, and organic compounds) for ZK were presented and discussed in details in our previous publications (Fadel et al., 2023; Fadel et al., 2021), and are resumed in **Table S2** and **Table S3.**

$PM_{2.5}$ average concentration for ZK was 33.6 µg.m^{-3}. The major chemical components were OC, EC, SO_4^{2-}, Ca, NH_4^+, and NO_3^- contributing to approximately 50% of the $PM_{2.5}$ mass **(Table S2)**. As for the organic compounds, hexa- and octadecanoic acids, tracers of cooking emissions, recorded the highest concentrations (259 and 175 ng/m^3, respectively) between the identified compounds, followed by levoglucosan (91 ng/m^3), tracer of biomass burning. The total concentrations of n-alkanes, PAHs, and hopanes were 26.7, 2.56, and 4.22, respectively **(Table S3)**.

Different organic and inorganic markers were used to estimate the contribution of the sources using the PMF source receptor model (Fadel et al., 2023). The chemical markers of the sources identified using PMF along with the average contributions of the sources to $PM_{2.5}$ during the entire sampling period as well as during winter and summer periods are presented in **Table 1**.

The average results show that 27.5% of $PM_{2.5}$ was attributed to crustal dust that mainly originate from the Arabian and Saharan deserts through long range transport (Fadel et al., 2023). Additionally, high concentrations of carbonaceous matter (OC and EC) were reported to be of long-range origins, possibly because of the abundance of oil fields and refineries in the surrounding Arab countries.

The ammonium sulfate source, which was the second highest contributor (15.7%), can be either of local (HFO combustion from the power plant) or distant origins (industrial areas of Europe and Turkey). The site was also influenced by vehicular emissions (14% of $PM_{2.5}$) with three PMF factors associated with exhaust and non-exhaust emissions **(Table 1)** since the site is close to a congested highway. Traffic exhaust (1) source, characterized by high loadings of 17α(H)-21β(H)-hopane is mainly associated to unburned lubricating oils while traffic exhaust (2) source is associated with high concentrations of OC and EC and is linked to fuel combustion.

Table 1: Markers of the identified sources at Zouk (ZK) site along with their average contribution to $PM_{2.5}$ in percentages and in $\mu g \cdot m^{-3}$ retrieved from Fadel et al. (2023) during the entire sampling period (Dec. 2018 – Nov. 2019), winter (Dec. 2018 – Mar. 2019), and summer (Jun. 2019 – Sept. 2019) periods.

Sources	Markers	Total period		Winter		Summer	
		Contrib. to $PM_{2.5}$ ($\mu g \cdot m^{-3}$)	Contrib. to $PM_{2.5}$ (%)	Contrib. to $PM_{2.5}$ ($\mu g \cdot m^{-3}$)	Contrib. to $PM_{2.5}$ (%)	Contrib. to $PM_{2.5}$ ($\mu g \cdot m^{-3}$)	Contrib. to $PM_{2.5}$ (%)
Crustal dust	Al, Ca, Mg, Ti, K	8.19	27.5%	10.52	40.8%	4.90	16.2%
Ammonium sulfate	SO_4^{2-}, NH_4^+	4.70	15.8%	2.10	8.2%	8.31	27.5%
HFO combustion	OC, EC, V, Ni	3.89	13.1%	1.39	5.4%	4.15	13.7%
Aged sea-salt	Na^+, Cl^-, NO_3^-	3.32	11.1%	2.27	8.8%	2.70	8.9%
Secondary biogenic	isoprene and α-pinene oxidation products	2.32	7.8%	0.40	1.5%	4.67	15.5%
Traffic exhaust (2)	OC, EC	1.83	6.1%	1.28	5.0%	2.15	7.1%
Traffic exhaust (1)	17α(H)-21β(H)-hopane	1.38	4.6%	2.12	8.2%	0.84	2.8%
Diesel generators	OC, EC, C_{20}, C_{21}	1.33	4.5%	1.73	6.7%	0.57	1.9%
Biomass burning	OC, EC, levoglucosan	1.03	3.4%	2.32	9.0%	0.07	0.2%
Traffic non-exhaust	Cu, Sb, Sn	0.99	3.3%	0.79	3.1%	0.93	3.1%
Primary biogenic	C_{27}, C_{29}, C_{31}	0.44	1.5%	0.50	2.0%	0.26	0.9%
Cooking	hexadecanoic and octadecanoic acids	0.42	1.4%	0.35	1.3%	0.67	2.2%

Furthermore, the industrial influence was highlighted by a relatively high contribution of HFO combustion from the power plant (13% of $PM_{2.5}$ mass). Biogenic sources (primary and secondary pathways) were also identified with a combined contribution of 9.3%, and aged sea-

256 salts contributed 11.1%. Other anthropogenic sources such as diesel generators, biomass burning,
257 and cooking emissions contributed together to 9.3% of $PM_{2.5}$ **(Table 1)**.

258

259 2.2 Oxidative potential of $PM_{2.5}$

260 The average volume and mass-normalized OP-AA and OP-DTT values at ZK are presented in
261 **Table 2** for the entire study period along with the values for winter and summer periods.
262 Additionally, time series for the different variables ($OP\text{-}AA_v$, $OP\text{-}AA_m$, $OP\text{-}DTT_v$, $OP\text{-}DTT_m$)
263 are presented in **Figure S1**. The mass-normalized OP corresponds to the intrinsic OP value
264 related to the oxidative properties of PM per unit mass while volume-normalized OP takes into
265 account the dilution of PM in the atmosphere and was considered to have a closer relation to
266 human exposure (Hakimzadeh et al., 2020).

267 The mean $OP\text{-}AA_v$ value at ZK was 0.64 ± 0.29 $nmol \cdot min^{-1} \cdot m^{-3}$, varying between 0.15 and 1.49
268 $nmol \cdot min^{-1} \cdot m^{-3}$ while the mean $OP\text{-}DTT_v$ value was 0.49 ± 0.26 $nmol \cdot min^{-1} \cdot m^{-3}$ with a minimum
269 of 0.12 and a maximum of 1.93 $nmol \cdot min^{-1} \cdot m^{-3}$. The values in our study for $OP\text{-}AA_v$ were in the
270 range of values reported for different urban and industrial sites in France such as Grenoble, Nice,
271 Talence, and Dunkirk (0.2-1.6 $nmol \cdot min^{-1} \cdot m^{-3}$) (Calas et al., 2019; Moufarrej et al., 2020).
272 Additionally, our values were higher than the ones reported for a Central Mediterranean
273 suburban site of the flat Salento's peninsula where $OP\text{-}AA_v$ average reported value was 0.29
274 $nmol \cdot min^{-1} \cdot m^{-3}$ (Pietrogrande et al., 2018) but in the same range of values reported for a
275 Mediterranean urban site in Spain (0.91 $nmol \cdot min^{-1} \cdot m^{-3}$) (Clemente et al., 2023).

276

277 **Table 2 :** Average volume (nmol·min^{-1}·m^{-3}) (OP-AA$_v$ and OP-DTT$_v$) and mass (nmol·min^{-1}·µg^{-1}) (OP-AA$_m$ and OP-DTT$_m$) normalized OP-AA and OP-DTT measured for $PM_{2.5}$ with their standard deviations for the total period, winter, and summer at Zouk (ZK) site.

	ZK site		
	Total Period	Winter	Summer
Periods	Dec. 2018 - Nov. 2019	Dec. 2018 - Mar. 2019	Jun. - Sept. 2019
OP-AA$_v$ (nmol·min^{-1}·m^{-3})	0.64 ± 0.29	0.70 ± 0.28	0.49 ± 0.14
OP-AA$_m$ (nmol·min^{-1}·µg^{-1})	0.03 ± 0.02	0.04 ± 0.02	0.02 ± 0.01
OP-DTT$_v$ (nmol·min^{-1}·m^{-3})	0.49 ± 0.26	0.43 ± 0.22	0.52 ± 0.21
OP-DTT$_m$ (nmol·min^{-1}·µg^{-1})	0.02 ± 0.01	0.02 ± 0.01	0.02 ± 0.01

280

281 As for DTT, the results of our study for OP-DTT$_v$ **(Table 2)** were in the range of values observed
282 over the southern United States (0.1-1.5 nmol·min^{-1}·m^{-3}), for French sites (0.36-4.12 nmol·min^{-1}·m^{-3}), and for Chinese sites (0.19-1.1 nmol·min^{-1}·m^{-3}) (Calas et al., 2019; Verma et al., 2014;
284 Wang et al., 2020). The average OP-AA$_m$ and OP-DTT$_m$ were 0.03 ± 0.02 and 0.02 ± 0.01
285 nmol·min^{-1}·µg^{-1}, and were also comparable to the values reported in the above-mentioned
286 studies. Despite the closeness in the average values of OP-AA$_v$ and OP-DTT$_v$, a different
287 temporal evolution is observed **(Figure S1).** This might be due to the specificity of each assay
288 towards certain $PM_{2.5}$ components.

289

290 2.3 Correlation between OP-AA$_v$ OP-DTT$_v$ and $PM_{2.5}$ chemical components

291 To investigate the relationships between OP values and species concentrations, Spearman
292 correlation coefficients between volume-normalized OP-AA or OP-DTT values and $PM_{2.5}$
293 components concentrations were calculated **(Table 3)**. The species include the carbonaceous

matter (OC, EC), water-soluble ions, elements, and different classes of organic compounds among which alkanes, polycyclic aromatic hydrocarbons (PAHs), hopanes, levoglucosan, carboxylic acids, and secondary compounds. This approach allows us to give insights into the species that might contribute to oxidative properties of PM.

OP-AA_v did not show a significant correlation with $PM_{2.5}$ concentration while OP-DTT_v is significantly correlated with $PM_{2.5}$ **(Table 3)**. Similar observations were done by Calas et al. (2019) and Yang et al. (2014) stressing on the idea that the OP values correlate more with specific species rather than $PM_{2.5}$ mass as a whole.

Both assays appeared sensitive to elements as observed in **Table 3**. However, organic compounds including hopanes, levoglucosan, alkanes, and PAHs were not found to correlate with OP-DTT_v. This is likely due to the fact that these water insoluble species may not serve as actual reactants in an aqueous solution (such as the Gamble's solution) to oxidize DTT (Bates et al., 2019; Fang et al., 2016). The same observations were presented by Liu et al. (2020) when examining the oxidative potential of PM in different areas in China. On the other hand, organic compounds showed significant correlations with OP-AA_v especially n-alkanes, PAHs, levoglucosan, and hopanes **(Table 3).** As for elements associated with crustal dust such as Al, Mg, K, and Ti, weak correlations were found for both assays. High concentrations of these crustal elements are usually predictive of long-range transport of dust from deserts in the Mediterranean region (Borgie et al., 2016). The occurrence of these phenomena were verified by the evaluation of the HYSPLIT backtrajectories showing air masses coming from Saharan and Arabian deserts to the sampling site (Fadel et al., 2023). A special attention was given to samples that verify these above-mentioned criteria in order to further understand the influence of dust storm episodes on OP values. For that purpose, samples that showed high concentrations of

crustal elements (or high contribution of the crustal dust source to $PM_{2.5}$) were reported **in Table S4** as well as their respective OP values with the comparison to the rest of the sampling period. OP-DTT_v average value for samples collected during dust storm episodes from Arabian or Saharan deserts (0.54 and 0.38 nmol·min^{-1}·m^{-3}, respectively) are not very different from the average of DTT_v of PM observed in the remaining sampling days (0.49 nmol·min^{-1}·m^{-3}) **(Table S4).** Similar conclusions were given by Chirizzi et al. (2017) that studied the influence of Saharan dust outbreaks on OP-DTT_v and did not find any significant differences between the average OP-DTT_v of PM in the area and the one from Saharan dust particles. Regarding OP-AA_v, the average value for samples collected during a Saharan dust outbreak (0.43 nmol·min^{-1}·m^{-3}) was slightly lower than the one reported for the remaining sampling days (0.62 nmol·min^{-1}·m^{-3}). However, a remarkable difference was observed when examining OP-AA_v values for samples under the influence of long-range transport from Arabian deserts presenting values (average of 1.05 nmol·min^{-1}·m^{-3}) that were 1.7 times higher than the average OP-AA_v for the rest of the sampling days. This might be explained by the higher concentrations of carbonaceous matter in $PM_{2.5}$ for the samples that were under the influence of Arabian deserts outbreaks (OC + EC: 10.2 μg·m^{-3}) in comparison with the samples under the influence of Saharan deserts (4.7 μg·m^{-3}) and the remaining sampling days (5.4 μg·m^{-3}) since it has been shown that the carbonaceous matter is well correlated with OP (Chirizzi et al., 2017; Moufarrej et al., 2020). It has been previously reported that in Fadel et al. (2023) that the higher concentrations of carbonaceous matter in these samples is due to their transportation with the dust from the numerous oil fields and refineries in Arab countries.

A strong correlation was found between OP-DTT_v and elements originating from different anthropogenic sources namely V, Ni, Zn, Cu, Sn, and Sb **(Table 3).** Elements such as Cu, V, and

Ni are known to be involved in the production of radicals via the Fenton reaction involving the reduction of H_2O_2 by a transition metal (Visentin et al., 2016) and control the DTT oxidation. Additionally, good and moderate correlations were found between OP-DTT_v and OC, and OP-DTT_v and EC, respectively. OC and EC were mainly attributed to vehicular emissions at the sampling site.

Cu, Sb, and Sn mainly originate from resuspension of road dust (non-exhaust vehicular emissions), while V and Ni are emitted by HFO combustion. Similar correlations were observed between OP-DTT_v and elements in Moufarrej et al. (2020) in Dunkirk, a coastal industrial city in Northern France. Moreover, OP-DTT_v did not show any significant correlation with PAHs that might be linked to vehicular emissions, in agreement with Vreeland et al. (2017).

On the other hand, OC, EC, many PAHs, and levoglucosan showed good correlations with OP-AAv. These results are in agreement with previous studies that showed a high sensitivity of OP-AAv assay to biomass burning and also to road traffic exhaust chemical markers (OC, EC, fluoranthene, pyrene, chrysene, benzo[a]pyrene) (Calas et al., 2018; Janssen et al., 2014; Moufarrej et al., 2020; Weber et al., 2021).

A strong correlation was also observed between OP-AA_v and indeno[1,2,3-c,d]pyrene that was linked to the HFO combustion from the power plant at ZK in our previous study (Fadel et al., 2021).OP-AA_v showed significant correlation with levoglucosan suggesting that biomass burning contributes to the value of OP-AA_v.

Table 3: Spearman correlation coefficient (r) between Oxidative Potential derived from AA and DTT depletion measurements ($OP\text{-}AA_v$ and $OP\text{-}DTT_v$), $PM_{2.5}$ concentrations, and $PM_{2.5}$ components (carbonaceous fraction, water-soluble ions, elements, and organic species) – Correlation coefficients for which p-value <0.05 are reported (*p<0.01; bold r>0.5).

	Species	$OP\text{-}AA_v$	$OP\text{-}DTT_v$
	$OP\text{-}AA_v$		0.41*
	$PM_{2.5}$		0.42*
Carbonaceous sub-fraction	OC	**0.53***	**0.51***
	EC	**0.53***	0.43*
Water-soluble ions	Cl^-		
	NO_3^-	0.28	0.21
	SO_4^{2-}		0.46*
	Na^+		
	NH_4^+		0.38*
	K^+	0.31	**0.53***
	Mg^{2+}		
	Ca^{2+}	0.21	0.26
Elements	Mg		0.23
	Mn	0.42*	0.31
	Al		
	Ba	0.35*	0.24
	Ca	0.22	0.23
	Fe	0.22	0.29
	K	0.26	0.39*
	Ni	0.47	**0.76***
	P	0.30	**0.52***
	V	0.29	**0.69***
	Pb	**0.52***	0.47*
	Sr		0.23
	Ti		0.23
	Zn	0.46	**0.67***
	Sc		
	Cr		
	Co	0.42*	0.46*
	Cu	0.38*	**0.50***
	As		0.47*
	Rb		0.31
	Nb		
	Cd	0.31	0.41*
	Sb	0.48*	**0.65***
	La		
	Ce		
	Tl		0.48*
	Bi		**0.50***

	Species	$OP\text{-}AA_v$	$OP\text{-}DTT_v$
n-alkanes	C_{19} – nonadecane	0.28	
	C_{20} – eicosane	0.29	
	C_{21}- heneicosane	0.41*	
	C_{22} - docosane	0.41*	
	C_{23} - tricosane	0.43*	
	C_{24} - tetracosane	0.43*	
	C_{25} - pentacosane	0.39*	
	C_{26} – hexacosane	0.39*	
	C_{27} - heptacosane	0.33*	
	C_{28} – octacosane	0.34*	
	C_{29} – nonacosane	0.25	
	C_{30} - triacontane	0.32	
	C_{31} - hentriacontane		0.21
	C_{32} - dotriacontane	0.25	0.29
PAHs	acenaphthylene	0.40*	
	acenaphthene	0.35*	
	fluorene	0.25	
	anthracene	0.46*	
	phenanthrene	**0.51***	
	fluoranthene	**0.50***	
	pyrene	**0.51***	
	benz[a]anthracene	**0.52***	
	chrysene	**0.56***	
	benzo[b]fluoranthene	**0.50***	
	benzo[k]fluoranthene	0.43*	
	benz[a]pyrene	**0.52***	
	dibenz[a,h]anthracene	**0.52***	
	benzo[g,h,i]perylene	0.45*	
	indeno[1,2,3-c,d]pyrene	**0.57***	
Anhydrosugar	levoglucosan	**0.50***	
Carboxylic acids	hexadecanoic acid		
	octadecanoic acid		
Secondary compounds	isoprene oxidation products		
	α-pinene oxidation products		
Hopanes	trisnorneohopane	0.23	
	17α(H)-trisnorhopane	0.32	
	17α(H)-21β(H)-norhopane	0.32	0.26
	17α(H)-21β(H)-hopane	0.36*	0.25
	17α(H)-21β(H)-22S-homohopane	0.26	0.24
	17α(H)-21β(H)-22R-homohopane		0.28

2.4 Apportionment of OP sources

2.4.1 Accuracy of the model

Once the initial MLR run was done, sources presenting negative intrinsic OP values and that were statistically unsignificant ($p < 0.05$) were removed from the initial input data and the MLR was done again. This was the case in our study for the "Cooking" source in OP-AA_v ($p = 0.547$) and for the "diesel generators" source in OP-DTT_v ($p = 0.07$). By that, the "cooking" source for OP-AA_v and the "diesel generators" source for OP-DTT_v will not be used in the source apportionment of OP.

The MLR was run again considering 11 sources instead of 12 for both assays. All the remaining sources for both assays showed positive intrinsic OP. A significant correlation was observed between the reconstructed and observed OP ($R^2>0.8$) with a regression line close to unity for both assays **(Figure S2).** The residuals between the observed and the modeled OP values were close to zero for low OP values and slightly increased for higher OP values **(Figure S3)**. Moreover, the distribution of the residuals is normal (Shapiro Wilk test, $p<0.05$) for both OP-AA and OP-DTT with a slight increase towards the underestimation for the highest OP values. All of these findings show that the modeling method is valid (Weber et al., 2021), and the results of intrinsic OP can be presented.

2.4.2 Intrinsic OP values

The values of intrinsic OP obtained from the base run as well as the median, 5^{th}, 25^{th}, 75^{th}, and 95^{th} percentile values of OP obtained from the bootstrap analysis are presented in **Figure 2**. The use of a boxplot representation allows to quickly evaluate the stability of the results: a certain confidence could be set on the intrinsic OP values showing low variability during the bootstrap procedure (25^{th} and 75^{th} percentile close to the median value). On the other hand, when 25^{th} et 75^{th} percentile values are far from the median values (high interquartile range), conclusions should be carefully drawn regarding the obtained intrinsic OP value for the considered sources.

For OP-AA_v, the bootstrap procedure evidenced few variabilities in the intrinsic OP for most of the sources. Additionally, the intrinsic OP values from the base run and median values from the bootstrap analysis were close **(Figure 2)**. For the majority of the identified sources, positive average intrinsic OP-AA values were observed stressing on the significant oxidative properties of PM. From the calculations, the biomass burning source showed the highest intrinsic OP with a value of 0.161 nmol·min^{-1}·μg^{-1}, followed by primary biogenic source (0.043 nmol·min^{-1}·μg^{-1}), HFO combustion (0.038 nmol·min^{-1}·μg^{-1}), traffic exhaust (2) (0.039 nmol·min^{-1}·μg^{-1}), diesel generators (0.037 nmol·min^{-1}·μg^{-1}), traffic exhaust (1) (0.035 nmol·min^{-1}·μg^{-1}), and then secondary biogenic source (0.015 nmol·min^{-1}·μg^{-1}). Biomass burning is one of the few sources that shows a considerably significant redox activity. Ammonium sulfate, aged sea-salt, and traffic non-exhaust sources showed considerably lower mean intrinsic OP-AA values (0.006 - 0.008 nmol·min^{-1}·μg^{-1}), and crustal dust source presented the lowest intrinsic OP-AA value (0.0002 nmol·min^{-1}·μg^{-1}) **(Figure 2)**.

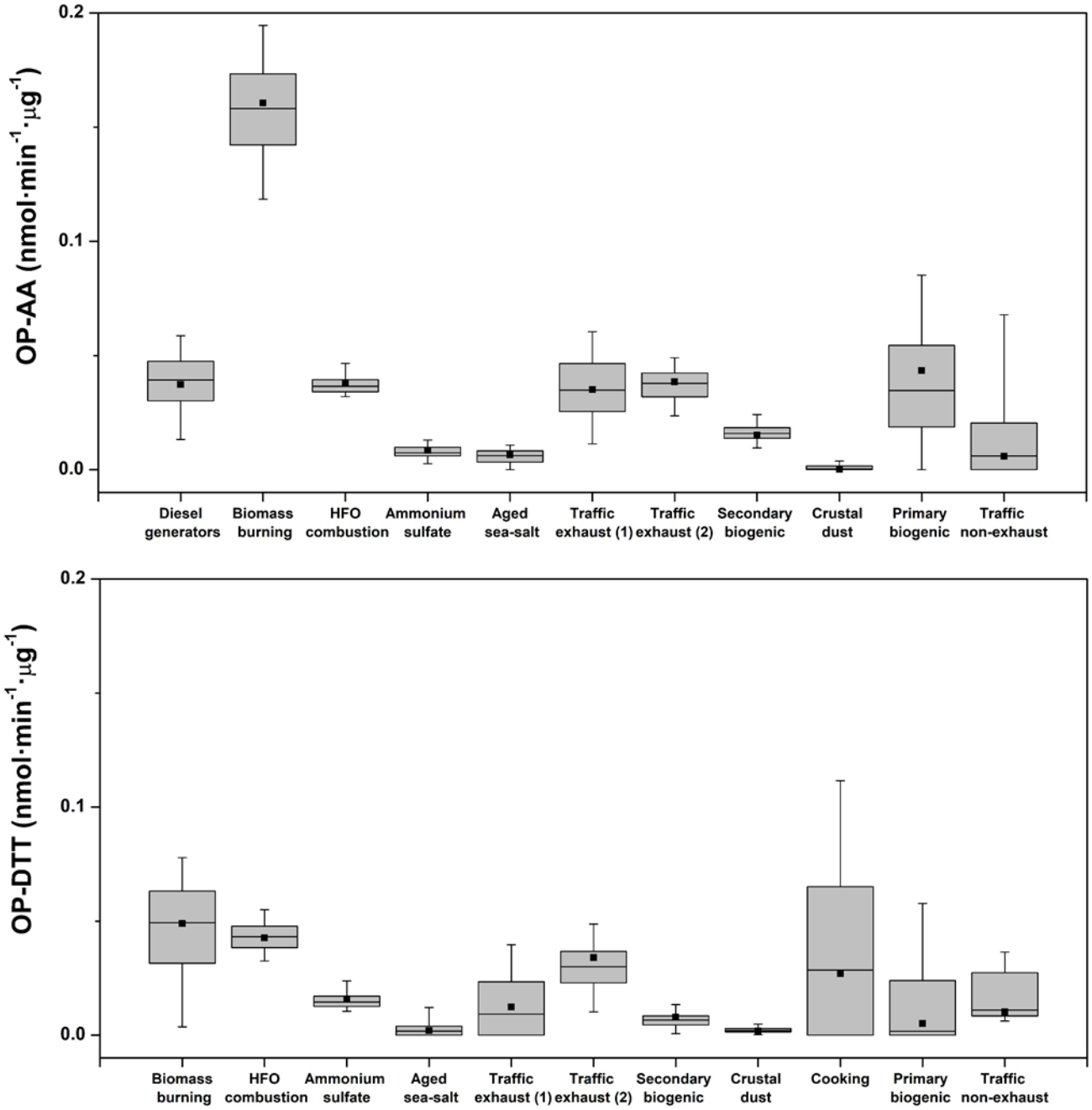

404

405 **Figure 2:** Boxplots of intrinsic OP values obtained from the bootstrap analysis for both AA and
406 DTT values expressed in nmol·min^{-1}·µg^{-1} (5th, 25th, 50th, 75th, and 95th percentiles) and the OP
407 value obtained from the base run for the identified sources by PMF at ZK (black squares).

For OP-DTT$_v$, the bootstrap method applied to the MLR results showed few variabilities for intrinsic OP values for most of the sources. The different sources also show close values between the obtained OP values from the base run and median values from the bootstrap analysis **(Figure 2)**. The highest variability of intrinsic OP-DTT values was observed for the cooking source. However, due to its low contribution to $PM_{2.5}$ (1.4%), it will not highly affect the apportionment results.

Biomass burning source showed the highest intrinsic OP-DTT$_v$ value (0.049 nmol·min^{-1}·µg^{-1}), followed by HFO combustion (0.043 nmol·min^{-1}·µg^{-1}), traffic exhaust (2) (0.034 nmol·min^{-1}·µg^{-1}), cooking (0.027 nmol·min^{-1}·µg^{-1}) ammonium sulfate (0.016 nmol·min^{-1}·µg^{-1}), traffic exhaust (1) (0.012 nmol·min^{-1}·µg^{-1}), and traffic non-exhaust (0.01 nmol·min^{-1}·µg^{-1}). Primary and secondary biogenic sources as well as crustal dust and aged sea-salt showed considerably lower intrinsic OP-DTT values (0.008-0.002 nmol·min^{-1}·µg^{-1}).

The examination of the intrinsic OP values reveals the sensitivity of the OP whether by AA or DTT measurements to PM sources and their chemical composition. Biomass burning source showed the highest intrinsic OP-AA value, that is at least three times higher than the value obtained for the HFO combustion and traffic exhaust sources. On the other hand, OP-DTT test seems to be multi-source influenced with close intrinsic values for biomass burning, HFO combustion, and traffic exhaust (2). Similar results were observed by Weber et al. (2018) when applying the method to the Chamonix site in France.

Furthermore, as observed earlier, sources with a high organic profile contribution show higher intrinsic values for AA test compared to DTT, namely biomass burning, secondary biogenic, diesel generators, and traffic exhaust (1) (having high loading of 17α(H)-21β(H)-hopane). As for HFO combustion source characterized by elements such as Ni and V, intrinsic OP values were

similar for both tests since AA and DTT are sensitive to elements, in line with the findings of Bates et al. (2019).

On the other hand, traffic non-exhaust characterized by high content of Cu, Sb, and Sn showed a strong variability in the MLR bootstrap results and its corresponding OP intrinsic values are relatively low compared to other sources **(Figure 2)**. Weber et al. (2018); (2021) presented intrinsic OP for elements associated to non-exhaust emissions in PM_{10}, but they were either combined to sea-salts or to carbonaceous matter related to exhaust vehicular emissions that largely contribute to the values of OP. The same observation was made in this study for the traffic exhaust (2) source, characterized by high loadings of OC and EC, and showed an intrinsic OP value for both assays. On the other hand, Shen et al. (2022) has highlighted the important contribution of brake and tire wear emissions to OP-DTT_v as the emitted elements could be redox-active. The low intrinsic OP values observed in our study for traffic non-exhaust might be linked to the PM fraction considered. Giannossa et al. (2022) have showed that resuspended dust mainly contributes to the OP of the coarse fraction rather than the fine one.

The ammonium sulfate source showed a significant intrinsic OP-DTT_v value as previously showed by Weber et al. (2018).

2.4.3 Contribution of the sources to the OP values

The average and normalized contribution of the sources to $PM_{2.5}$ concentration, OP-AA_v, and OP-DTT_v for the total period as well as for winter and summer periods are presented in **Figure 3**. Source contribution was calculated for all the sources except for the “cooking” source for OP-AA_v and the “diesel generators” source for OP-DTT_v. The “unexplained” category corresponds

to the difference between the observed OP and the sum of the contributions of all the sources. For the total period, 95% of OP-AA_v and 88% of OP-DTT_v observed values could be explained by the identified sources.

It can be directly observed that the sources that largely contribute to $PM_{2.5}$ in the total period were not the ones contributing the most to the OP values. Specifically, crustal dust source, that contributes to 27.5% of $PM_{2.5}$, only contributes to 3.3% of OP-DTT_v and to 0.3% of OP-AA_v.

The second contributor to $PM_{2.5}$ is the ammonium sulfate source (15.8% of $PM_{2.5}$) that contributes to 6.3% of OP-AA_v and 15.4% of OP-DTT_v. In different studies, it has been reported that secondary inorganic sources, such as ammonium sulfate and ammonium nitrate, are commonly associated with low toxicity in PM, and their ions do not exhibit any sensitivity towards both AA and DTT assays (Borlaza et al., 2021; Calas et al., 2019; Cesari et al., 2019; Verma et al., 2014). However, the contribution of the ammonium sulfate source to OP-DTT_v might be attributed to the formation of redox active SOA at the same time as the inorganic ions. In this study, the ammonium sulfate factor identified by PMF is mainly associated with the HFO combustion from the power plant in addition to distant sources (through long-range transport) from Turkey and Western Europe during late spring and summer seasons (Fadel et al., 2023). This source represents by that a regional secondary factor with an anthropogenic influence that could explain its contribution to OP, particularly OP-DTT. Weber et al. (2021) have also reported a considerable intrinsic OP value for the ammonium sulfate source, identified through 7500 samples, in the DTT assay due to the presence of organic carbon in the chemical profile.

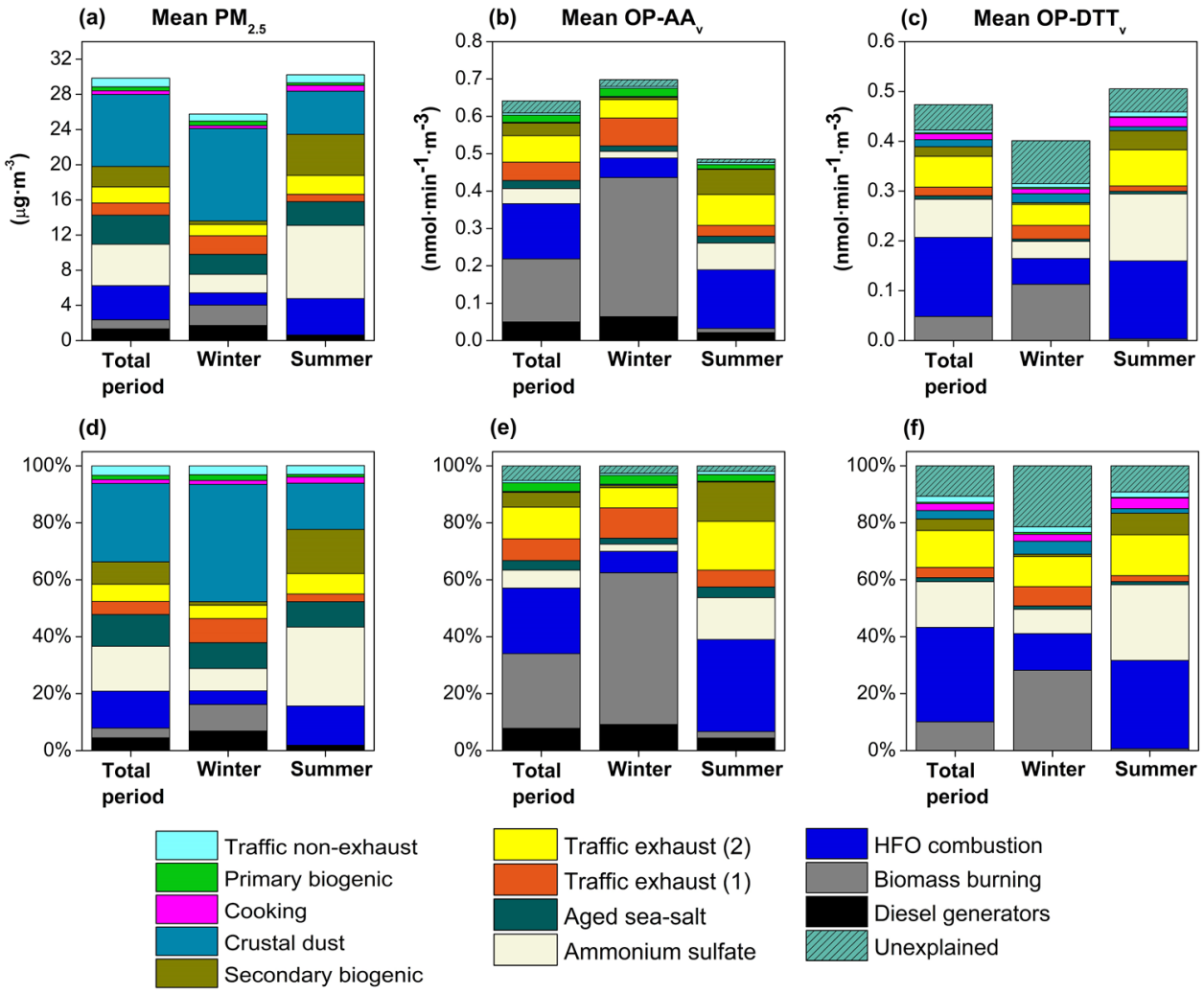

472

473

474 **Figure 3:** Mean contribution of the sources to the (a) $PM_{2.5}$ concentration, (b) OP-AA_v, and (c)
475 OP-DTT_v for the total (Dec 2018-Nov 2019), winter (Dec 2018-March 2019), and summer (June
476 2019-September 2019) periods; their respective normalized contributions are presented for (d)
477 $PM_{2.5}$ concentration, (e) OP-AA_v, and (f) OP-DTT_v for the different periods.

478

479 Biomass burning which was only responsible for 3.4% of $PM_{2.5}$ also shows a low contribution to
480 OP-DTT_v (10.3%), but the highest share of OP-AA_v between the sources (26.3%). Traffic

exhaust and non-exhaust emission sources contribute to both OP-AA_v and OP-DTT_v with a share of 19.5% and 18.4%, respectively. As for the industrial typology of the site, HFO combustion attributed to the power plant showed high shares to both assays with a contribution of 23.1% for OP-AA_v and 32.7% for OP-DTT_v **(Figure 3)**.

We can conclude that common sources contribute the most to the values of OP, namely biomass burning, traffic emissions, and HFO combustion explaining 69% of OP-AA_v value and 62% of OP-DTT_v. These results were consistent with several literature studies that report dominant contribution of biomass burning to OP-DTT_v and OP-AA_v, (Fang et al., 2016; Perrone et al., 2019; Verma et al., 2014), traffic emissions as well as fuel oil combustion (Crobeddu et al., 2017; Moreno et al., 2017; Yang et al., 2014). Primary and secondary biogenic sources contribute to 8.2% of OP-AA_v value and 4.4% of OP-DTT_v while aged sea-salts contribute to 3.4% of OP-AA_v and 1.4% of OP-DTT_v. Diesel generator contributed to 7.8% of OP-AA_v and the cooking emissions source contribute to 2.4% of OP-DTT_v.

2.5 Seasonal variations

When comparing winter and summer periods, the overall OP-DTT_v did not show any significant variability ($p>0.05$). However, a different scenario was observed for OP-AA_v since the values were significantly higher ($p<0.001$) during winter period compared to summer (**Table 2)**. According to the literature, there is not a unique trend for the seasonal variations either for OP-DTT or OP-AA. Several papers have reported a strong seasonality of OP with higher values during winter compared to summer (Borlaza et al., 2021; Calas et al., 2019; Calas et al., 2018; Verma et al., 2014) while others have presented the opposite seasonal trend (Charrier et al.,

2015; Fang et al., 2016; Perrone et al., 2016). In the same context, Pietrogrande et al. (2019) have reported that observed OP-DTT values were independent from seasonality in different rural and urban sites. Additionally, different seasonal trends might be observed for different PM fractions. For instance, Giannossa et al. (2022) showed that higher OP-DTT_v were observed during summer for $PM_{10-2.5}$ fraction while higher values were observed during winter for $PM_{2.5}$, suggesting that different sources with different seasonality might influence OP-DTT_v.

These observations might lead to the conclusion that the OP is significantly correlated with the chemical composition of PM and its temporal variability is linked to the emission sources and their intensities that are different across sampling sites.

In this work, the results presented in **Figure 3** revealed significant differences in the contributions of the sources especially for biomass burning and HFO combustion between winter and summer periods. The biomass burning source, contributing only to 9.0% of $PM_{2.5}$ during winter, was found to be the major contributor to both OP-AA_v (53.3%) and OP-DTT_v (26.5%). These contributions were 33 and 34 times higher than the ones observed during summer for OP-AA_v (2.3%) and OP-DTT_v (0.7%), respectively **(Figure 3)**. This predominance of biomass burning source to OP values during cold months has been previously reported in the literature by Borlaza et al. (2021) and Verma et al. (2014) and highlights the severity of biomass burning emissions from residential heating during the winter. On the other hand, the HFO combustion source from the power plant demonstrated higher contributions during the warm period for OP-AAv (32.3%) and for OP-DTTv (31%) compared to the cold period (7.5% for OP-AAv and 14.2% for OP-DTTv). This might be attributed to the increase in electricity production during the summer months, which leads to a higher contribution of this source to $PM_{2.5}$ (13.7% during summer vs. 5.4% during winter). In contrast, the contributions from traffic sources were found to

be relatively consistent throughout the year, with variations of less than 6% **(Figure 3)**. Additionally, secondary biogenic source was found to have at least 10 times higher contribution to both OP assays during the summer compared to winter. Ammonium sulfate sources showed considerably higher contribution to OP-DTT_v during summer (26.6% vs. 8.0% during winter) due to the higher contribution of the source to $PM_{2.5}$ **(Table 1)**.

As previously mentioned, the ammonium sulfate is mainly emitted from the HFO combustion from the power plant in addition to distant anthropogenic sources that arrive to the site through long range transport especially during summer (Fadel et al., 2023).

3 Conclusion

This work represents a significant advancement in the field of air quality research in the East Mediterranean and the Middle East region. Specifically, this work focused on evaluating the oxidative potential (OP) of $PM_{2.5}$ samples collected for almost a year (December 2018 - October 2019) using two acellular assays: ascorbic acid (AA) and dithiothreitol (DTT), correlating OP values with a wide range of chemical species in $PM_{2.5}$, and on apportioning OP on different emission sources. The mean OP-AA_v value was 0.64 ± 0.29 $nmol \cdot min^{-1} \cdot m^{-3}$ and the mean OP-DTT_v was 0.49 ± 0.26 $nmol \cdot min^{-1} \cdot m^{-3}$. Spearman correlations showed that OP-AA_v showed strong correlations with the carbonaceous subfractions, and organic compounds while OP-DTT_v showed a strong correlation with elements emitted from anthropogenic activities such as V, Ni, Zn, Cu, Sn, and Sb.

A multiple linear regression method was applied in order to estimate the contribution of PM sources to the OP values. The results showed that crustal dust and ammonium sulfate sources

548 that largely contribute to $PM_{2.5}$ mass were not the major sources contributing to the values of OP.
549 However, 69% of OP-AA_v and 62% of OP-DTT_v values were explained by three local
550 anthropogenic sources: Heavy Fuel Oil (HFO) combustion from a power plant, biomass burning,
551 and road traffic emissions. Seasonal variations showed that biomass burning is the largest
552 contributor to OP during winter (53.3% for OP-AA_v and 26.5% for OP-DTT_v) while HFO
553 combustion contributes the most during summer (32.3% for OP-AA_v, and 31% for OP-DTT_v). In
554 contrast, the contributions from traffic sources were found to be relatively consistent throughout
555 the year (18% and 24% of OP-AA_v and 18% and 19% of OP-DTT_v during winter and summer,
556 respectively). Following the obtained results, air quality plans should be prioritizing these three
557 sources to limit the impact of air pollution on human health. Overall, this study has provided
558 insight into the relationship between PM sources and oxidative potential in an urban site in the
559 East Mediterranean.

560

561 Acknowledgment:

562 The authors would like to acknowledge the National Council for Scientific Research of Lebanon
563 (CNRS-L) and Université du Littoral Cote d'Opale (ULCO) for granting a doctoral fellowship to
564 Marc Fadel. This project was also funded by the Research Council and the Faculty of Sciences of
565 Saint Joseph University of Beirut – Lebanon. The "Unité de Chimie Environnementale et
566 Interactions sur le Vivant" (UCEIV-UR4492) participates in the CLIMIBIO project, which is
567 financially supported by the Hauts-de-France Region Council, the French Ministry of Higher
568 Education and Research, and the European Regional Development Funds. This publication has
569 been also produced within the framework of the EMME-CARE project, which has received

570 funding from the European Union's Horizon 2020 Research and Innovation Programme (under
571 grant agreement no. 856612) and the Cyprus Government.

572 The authors thank Institut Chevreul - Université de Lille for the analysis of elements by ICP-MS
573 and The Cyprus Institute for the OC/EC analysis. The authors would also like to thank Dorothée
574 Dewaele (Centre Commun de Mesures, ULCO) for her help in the ICP-AES analysis, Amaury
575 Kasprowiak and Marianne Seigneur for their help in the ionic chromatography analysis, and
576 Mariana Farhat for her help in the organic fraction analysis.

577

578 References:

579 Anderson JO, Thundiyil JG, Stolbach A. Clearing the air: a review of the effects of particulate
580 matter air pollution on human health. J Med Toxicol 2012; 8: 166-
581 175.https://10.1007/s13181-011-0203-1.

582 Ayres JG, Borm P, Cassee FR, Castranova V, Donaldson K, Ghio A, Harrison RM, Hider R,
583 Kelly F, Kooter IM, Marano F, Maynard RL, Mudway I, Nel A, Sioutas C, Smith S,
584 Baeza-Squiban A, Cho A, Duggan S, Froines J. Evaluating the Toxicity of Airborne
585 Particulate Matter and Nanoparticles by Measuring Oxidative Stress Potential—A
586 Workshop Report and Consensus Statement. Inhal Tox 2008; 20: 75-
587 99.https://doi.org/10.1080/08958370701665517.

588 Bates JT, Fang T, Verma V, Zeng L, Weber RJ, Tolbert PE, Abrams JY, Sarnat SE, Klein M,
589 Mulholland JA, Russell AG. Review of acellular assays of ambient particulate matter
590 oxidative potential: Methods and relationships with composition, sources, and health

effects. Environ Sci Technol 2019; 53: 4003-4019.https://doi.org/10.1021/acs.est.8b03430.

Bates JT, Weber RJ, Abrams J, Verma V, Fang T, Klein M, Strickland MJ, Sarnat SE, Chang HH, Mulholland JA, Tolbert PE, Russell AG. Reactive oxygen species generation linked to sources of atmospheric particulate matter and cardiorespiratory effects. Environ. Sci. Tech. 2015; 49: 13605-13612.https://doi.org/10.1021/acs.est.5b02967.

Becker S, Dailey LA, Soukup JM, Grambow SC, Devlin RB, Huang Y-CT. Seasonal variations in air pollution particle-induced inflammatory mediator release and oxidative stress. Environ. Health Perspect. 2005; 113: 1032-1038.https://doi.org/10.1289/ehp.7996.

Borgie M, Ledoux F, Dagher Z, Verdin A, Cazier F, Courcot L, Shirali P, Greige-Gerges H, Courcot D. Chemical characteristics of $PM_{2.5–0.3}$ and $PM_{0.3}$ and consequence of a dust storm episode at an urban site in Lebanon. Atmos Res 2016; 180: 274-286.https://doi.org/10.1016/j.atmosres.2016.06.001.

Borlaza LJS, Weber S, Jaffrezo JL, Houdier S, Slama R, Rieux C, Albinet A, Micallef S, Trébluchon C, Uzu G. Disparities in particulate matter (PM_{10}) origins and oxidative potential at a city scale (Grenoble, France) – Part 2: Sources of PM_{10} oxidative potential using multiple linear regression analysis and the predictive applicability of multilayer perceptron neural network analysis. Atmos. Chem. Phys. 2021; 21: 9719-9739.https://doi.org/10.5194/acp-21-9719-2021.

Calas A, Uzu G, Besombes J-L, Martins JMF, Redaelli M, Weber S, Charron A, Albinet A, Chevrier F, Brulfert G, Mesbah B, Favez O, Jaffrezo J-L. Seasonal variations and

chemical predictors of oxidative potential (OP) of particulate matter (PM), for seven urban French sites. Atmosphere 2019; 10: 698.https://doi.org/10.3390/atmos10110698.

Calas A, Uzu G, Kelly FJ, Houdier S, Martins JMF, Thomas F, Molton F, Charron A, Dunster C, Oliete A, Jacob V, Besombes JL, Chevrier F, Jaffrezo JL. Comparison between five acellular oxidative potential measurement assays performed with detailed chemistry on PM_{10} samples from the city of Chamonix (France). Atmos. Chem. Phys. 2018; 18: 7863-7875.https://doi.org/10.5194/acp-18-7863-2018.

Cavalli F, Viana M, Yttri KE, Genberg J, Putaud JP. Toward a standardised thermal-optical protocol for measuring atmospheric organic and elemental carbon: the EUSAAR protocol. Atmos. Meas. Tech. 2010; 3: 79-89.https://doi.org/10.5194/amt-3-79-2010.

Cesari D, Merico E, Grasso FM, Decesari S, Belosi F, Manarini F, De Nuntiis P, Rinaldi M, Volpi F, Gambaro A, Morabito E, Contini D. Source Apportionment of PM2.5 and of its Oxidative Potential in an Industrial Suburban Site in South Italy. Atmosphere 2019; 10: 758

Charrier JG, Richards-Henderson NK, Bein KJ, McFall AS, Wexler AS, Anastasio C. Oxidant production from source-oriented particulate matter – Part 1: Oxidative potential using the dithiothreitol (DTT) assay. Atmos. Chem. Phys. 2015; 15: 2327-2340.10.5194/acp-15-2327-2015.

Chirizzi D, Cesari D, Guascito MR, Dinoi A, Giotta L, Donateo A, Contini D. Influence of Saharan dust outbreaks and carbon content on oxidative potential of water-soluble

fractions of $PM_{2.5}$ and PM_{10}. Atmos. Environ. 2017; 163: 1-8.https://doi.org/10.1016/j.atmosenv.2017.05.021.

Cho AK, Sioutas C, Miguel AH, Kumagai Y, Schmitz DA, Singh M, Eiguren-Fernandez A, Froines JR. Redox activity of airborne particulate matter at different sites in the Los Angeles Basin. Environ Res 2005; 99: 40-7.https://doi.org/10.1016/j.envres.2005.01.003.

Clemente Á, Gil-Moltó J, Yubero E, Juárez N, Nicolás JF, Crespo J, Galindo N. Sensitivity of PM10 oxidative potential to aerosol chemical composition at a Mediterranean urban site: ascorbic acid versus dithiothreitol measurements. Air Quality, Atmosphere & Health 2023.10.1007/s11869-023-01332-1.

Colombo C, Monhemius AJ, Plant JA. Platinum, palladium and rhodium release from vehicle exhaust catalysts and road dust exposed to simulated lung fluids. Ecotoxicol. Environ. Saf. 2008; 71: 722-730.https://doi.org/10.1016/j.ecoenv.2007.11.011.

Crobeddu B, Aragao-Santiago L, Bui L-C, Boland S, Baeza Squiban A. Oxidative potential of $PM_{2.5}$ as predictive indicator of cellular stress. Environ. Pollut. 2017; 230: 125-133.https://doi.org/10.1016/j.envpol.2017.06.051.

Daellenbach KR, Uzu G, Jiang J, Cassagnes L-E, Leni Z, Vlachou A, Stefenelli G, Canonaco F, Weber S, Segers A, Kuenen JJP, Schaap M, Favez O, Albinet A, Aksoyoglu S, Dommen J, Baltensperger U, Geiser M, El Haddad I, Jaffrezo J-L, Prévôt ASH. Sources of particulate-matter air pollution and its oxidative potential in Europe. Nature 2020; 587: 414-419.https://doi.org/10.1038/s41586-020-2902-8.

652 Fadel M, Courcot D, Delmaire G, Roussel G, Afif C, Ledoux F. Source apportionment of $PM_{2.5}$
653 oxidative potential in an East Mediterranean site. Submitted. Sci. Total Environ. 2023

654 Fadel M, Ledoux F, Afif C, Courcot D. Human health risk assessment for PAHs, phthalates,
655 elements, PCDD/Fs, and DL-PCBs in $PM_{2.5}$ and for NMVOCs in two East-
656 Mediterranean urban sites under industrial influence. Atmos. Pollut. Res. 2022; 13:
657 101261.https://doi.org/10.1016/j.apr.2021.101261.

658 Fadel M, Ledoux F, Farhat M, Kfoury A, Courcot D, Afif C. $PM_{2.5}$ characterization of primary
659 and secondary organic aerosols in two urban-industrial areas in the East Mediterranean. J.
660 Environ. Sci. 2021; 101: 98-116.https://doi.org/10.1016/j.jes.2020.07.030.

661 Fakhri N, Fadel M, Pikridas M, Sciare J, Hayes PL, Afif C. Source apportionment of PM2.5
662 using organic/inorganic markers and emission inventory evaluation in the East
663 Mediterranean-Middle East city of Beirut. Environmental Research 2023; 223:
664 115446.https://doi.org/10.1016/j.envres.2023.115446.

665 Fang T, Verma V, Bates JT, Abrams J, Klein M, Strickland MJ, Sarnat SE, Chang HH,
666 Mulholland JA, Tolbert PE, Russell AG, Weber RJ. Oxidative potential of ambient
667 water-soluble $PM_{2.5}$ in the southeastern United States: contrasts in sources and health
668 associations between ascorbic acid (AA) and dithiothreitol (DTT) assays. Atmos. Chem.
669 Phys. 2016; 16: 3865-3879.https://doi.org/10.5194/acp-16-3865-2016.

670 Giannossa LC, Cesari D, Merico E, Dinoi A, Mangone A, Guascito MR, Contini D. Inter-annual
671 variability of source contributions to PM_{10}, $PM_{2.5}$, and oxidative potential in an urban

672 background site in the central mediterranean. Journal of Environmental Management
673 2022; 319: 115752.https://doi.org/10.1016/j.jenvman.2022.115752.

674 Guascito MR, Lionetto MG, Mazzotta F, Conte M, Giordano ME, Caricato R, De Bartolomeo
675 AR, Dinoi A, Cesari D, Merico E, Mazzotta L, Contini D. Characterisation of the
676 correlations between oxidative potential and in vitro biological effects of PM_{10} at three
677 sites in the central Mediterranean. Journal of Hazardous Materials 2023; 448:
678 130872.https://doi.org/10.1016/j.jhazmat.2023.130872.

679 Guo H, Jin L, Huang S. Effect of PM characterization on PM oxidative potential by acellular
680 assays: a review. Rev. Environ. Health . 2020; 35: 461-470.https://doi.org/10.1515/reveh-
681 2020-0003.

682 Hakimzadeh M, Soleimanian E, Mousavi A, Borgini A, De Marco C, Ruprecht AA, Sioutas C.
683 The impact of biomass burning on the oxidative potential of $PM_{2.5}$ in the metropolitan
684 area of Milan. Atmos. Environ. 2020; 224:
685 117328.https://doi.org/10.1016/j.atmosenv.2020.117328.

686 Janssen NAH, Yang A, Strak M, Steenhof M, Hellack B, Gerlofs-Nijland ME, Kuhlbusch T,
687 Kelly F, Harrison R, Brunekreef B, Hoek G, Cassee F. Oxidative potential of particulate
688 matter collected at sites with different source characteristics. Sci. Total Environ. 2014;
689 472: 572-581.https://doi.org/10.1016/j.scitotenv.2013.11.099.

690 Ledoux F, Courcot L, Courcot D, Aboukaïs A, Puskaric E. A summer and winter apportionment
691 of particulate matter at urban and rural areas in northern France. Atmos. Res. 2006a; 82:
692 633-642.https://doi.org/10.1016/j.atmosres.2006.02.019.

693 Ledoux F, Laversin H, Courcot D, Courcot L, Zhilinskaya EA, Puskaric E, Aboukaïs A.
694 Characterization of iron and manganese species in atmospheric aerosols from
695 anthropogenic sources. Atmos. Res. 2006b; 82: 622-
696 632.https://doi.org/10.1016/j.atmosres.2006.02.018.

697 Lelieveld J, Klingmüller K, Pozzer A, Pöschl U, Fnais M, Daiber A, Münzel T. Cardiovascular
698 disease burden from ambient air pollution in Europe reassessed using novel hazard ratio
699 functions. Eur. Heart J. 2019; 40: 1590-1596.https://doi.org/10.1093/eurheartj/ehz135.

700 Lelieveld J, Münzel T. Air pollution, the underestimated cardiovascular risk factor. Eur. Heart J.
701 2020; 41: 904-905.https://doi.org/10.1093/eurheartj/ehaa063.

702 Liu Q, Lu Z, Xiong Y, Huang F, Zhou J, Schauer JJ. Oxidative potential of ambient $PM_{2.5}$ in
703 Wuhan and its comparisons with eight areas of China. Sci. Total Environ. 2020; 701:
704 134844.https://doi.org/10.1016/j.scitotenv.2019.134844.

705 Moreno T, Kelly FJ, Dunster C, Oliete A, Martins V, Reche C, Minguillón MC, Amato F,
706 Capdevila M, de Miguel E, Querol X. Oxidative potential of subway $PM_{2.5}$. Atmos.
707 Environ. 2017; 148: 230-238.https://doi.org/10.1016/j.atmosenv.2016.10.045.

708 Moufarrej L, Courcot D, Ledoux F. Assessment of the $PM_{2.5}$ oxidative potential in a coastal
709 industrial city in Northern France: Relationships with chemical composition, local
710 emissions and long range sources. Sci. Total Environ. 2020; 748:
711 141448.https://doi.org/10.1016/j.scitotenv.2020.141448.

712 Mudway IS, Stenfors N, Duggan ST, Roxborough H, Zielinski H, Marklund SL, Blomberg A,
713 Frew AJ, Sandström T, Kelly FJ. An in vitro and in vivo investigation of the effects of

diesel exhaust on human airway lining fluid antioxidants. Arch Biochem Biophys 2004; 423: 200-12.https://doi.org/10.1016/j.abb.2003.12.018.

Paatero P, Tapper U. Positive matrix factorization: A non-negative factor model with optimal utilization of error estimates of data values. Environmetrics 1994; 5: 111-126.https://doi.org/10.1002/env.3170050203.

Perrone M, Bertoli I, Romano S, Russo M, Rispoli G, Pietrogrande M. $PM_{2.5}$ and PM_{10} oxidative potential at a Central Mediterranean Site: Contrasts between dithiothreitol- and ascorbic acid-measured values in relation with particle size and chemical composition. Atmos. Environ. 2019; 210.https://doi/org/10.1016/j.atmosenv.2019.04.047.

Perrone MG, Zhou J, Malandrino M, Sangiorgi G, Rizzi C, Ferrero L, Dommen J, Bolzacchini E. PM chemical composition and oxidative potential of the soluble fraction of particles at two sites in the urban area of Milan, Northern Italy. Atmos. Environ. 2016; 128: 104-113.https://doi.org/10.1016/j.atmosenv.2015.12.040.

Pietrogrande M, Russo, Zagatti. Review of PM Oxidative Potential Measured with Acellular Assays in Urban and Rural Sites across Italy. Atmosphere 2019; 10: 626.10.3390/atmos10100626.

Pietrogrande MC, Perrone MR, Manarini F, Romano S, Udisti R, Becagli S. PM_{10} oxidative potential at a Central Mediterranean Site: Association with chemical composition and meteorological parameters. Atmos. Environ. 2018; 188: 97-111.https://doi.org/10.1016/j.atmosenv.2018.06.013.

Politis DN, White H. Automatic block-length selection for the dependent bootstrap. Econometric Reviews 2004; 23: 53-70.https://doi.org/10.1081/ETC-120028836.

Saffari A, Daher N, Shafer MM, Schauer JJ, Sioutas C. Seasonal and spatial variation in dithiothreitol (DTT) activity of quasi-ultrafine particles in the Los Angeles Basin and its association with chemical species. Journal of environmental science and health. Part A, Toxic/hazardous substances & environmental engineering 2014; 49: 441-51.https://doi.org/10.1080/10934529.2014.854677.

Serafeim E, Besis A, Kouras A, Farias CN, Yera AB, Pereira GM, Samara C, de Castro Vasconcellos P. Oxidative potential of ambient PM2.5 from São Paulo, Brazil: Variations, associations with chemical components and source apportionment. Atmos. Environ. 2023; 298: 119593.https://doi.org/10.1016/j.atmosenv.2023.119593.

Shen J, Taghvaee S, La C, Oroumiyeh F, Liu J, Jerrett M, Weichenthal S, Del Rosario I, Shafer MM, Ritz B, Zhu Y, Paulson SE. Aerosol oxidative potential in the Greater Los Angeles area: Source apportionment and associations with socioeconomic position. Environ Sci Technol 2022; 56: 17795-17804.https://doi.org/10.1021/acs.est.2c02788.

Verma V, Fang T, Guo H, King L, Bates JT, Peltier RE, Edgerton E, Russell AG, Weber RJ. Reactive oxygen species associated with water-soluble $PM_{2.5}$ in the southeastern United States: spatiotemporal trends and source apportionment. Atmos. Chem. Phys. 2014; 14: 12915-12930.https://doi.org/10.5194/acp-14-12915-2014.

753 Visentin M, Pagnoni A, Sarti E, Pietrogrande MC. Urban $PM_{2.5}$ oxidative potential: Importance
754 of chemical species and comparison of two spectrophotometric cell-free assays. Environ.
755 Pollut. 2016; 219: 72-79.https://doi.org/10.1016/j.envpol.2016.09.047.

756 Vreeland H, Weber R, Bergin M, Greenwald R, Golan R, Russell AG, Verma V, Sarnat JA.
757 Oxidative potential of $PM_{2.5}$ during Atlanta rush hour: Measurements of in-vehicle
758 dithiothreitol (DTT) activity. Atmos. Environ. 2017; 165: 169-
759 178.https://doi.org/10.1016/j.atmosenv.2017.06.044.

760 Wang J, Lin X, Lu L, Wu Y, Zhang H, Lv Q, Liu W, Zhang Y, Zhuang S. Temporal variation of
761 oxidative potential of water soluble components of ambient $PM_{2.5}$ measured by
762 dithiothreitol (DTT) assay. Sci. Total Environ. 2019; 649: 969-
763 978.https://doi.org/10.1016/j.scitotenv.2018.08.375.

764 Wang Y, Wang M, Li S, Sun H, Mu Z, Zhang L, Li Y, Chen Q. Study on the oxidation potential
765 of the water-soluble components of ambient $PM_{2.5}$ over Xi'an, China: Pollution levels,
766 source apportionment and transport pathways. Environ. Int. 2020; 136:
767 105515.https://doi.org/10.1016/j.envint.2020.105515.

768 Weber S, Uzu G, Calas A, Chevrier F, Besombes JL, Charron A, Salameh D, Ježek I, Močnik G,
769 Jaffrezo JL. An apportionment method for the oxidative potential of atmospheric
770 particulate matter sources: application to a one-year study in Chamonix, France. Atmos.
771 Chem. Phys. 2018; 18: 9617-9629.https://doi.org/10.5194/acp-18-9617-2018.

772 Weber S, Uzu G, Favez O, Borlaza LJS, Calas A, Salameh D, Chevrier F, Allard J, Besombes J-
773 L, Albinet A, Pontet S, Mesbah B, Gille G, Zhang S, Pallares C, Leoz-Garziandia E,

774 Jaffrezo J-L. Source apportionment of atmospheric PM_{10} oxidative potential: synthesis of
775 15 year-round urban datasets in France. Atmos. Chem. Phys. 2021; 21: 11353-
776 11378.https://doi.org/10.5194/acp-21-11353-2021.

777 WHO, 2021. WHO air quality guidelines. Particulate matter ($PM_{2.5}$ and PM_{10}), ozone, nitrogen
778 dioxide, sulfur dioxide and carbon monoxide. Geneva: World Health Organization
779 Switzerland. Licence: CC BY-NC-SA 3.0 IGO.,

780 Xing Y-F, Xu Y-H, Shi M-H, Lian Y-X. The impact of $PM_{2.5}$ on the human respiratory system. J
781 Thorac Dis 2016; 8: E69-E74.https://doi.org/10.3978/j.issn.2072-1439.2016.01.19.

782 Xu F, Shi X, Qiu X, Jiang X, Fang Y, Wang J, Hu D, Zhu T. Investigation of the chemical
783 components of ambient fine particulate matter ($PM_{2.5}$) associated with in vitro cellular
784 responses to oxidative stress and inflammation. Environ. Int. 2020; 136:
785 105475.https://doi.org/10.1016/j.envint.2020.105475.

786 Yang A, Jedynska A, Hellack B, Kooter I, Hoek G, Brunekreef B, Kuhlbusch TAJ, Cassee FR,
787 Janssen NAH. Measurement of the oxidative potential of $PM_{2.5}$ and its constituents: The
788 effect of extraction solvent and filter type. Atmos. Environ. 2014; 83: 35-
789 42.https://doi.org/10.1016/j.atmosenv.2013.10.049.

790